

# An electron momentum spectroscopy and density functional theory investigation into the complete valence electronic structure of ethylene oxide

D A Winkler<sup>†</sup>, M T Michalewicz<sup>‡</sup>, F Wang<sup>§</sup> and M J Brunger<sup>¶</sup>

<sup>†</sup> Division of Molecular Science, CSIRO, Private Bag 10, Clayton, Victoria 3168, Australia

<sup>‡</sup> CSIRO Mathematical and Information Sciences, BoM/CSIRO High Performance Computing and Communication Centre, 24th Floor, 150 Lonsdale Street, Melbourne, Victoria 3000, Australia

<sup>§</sup> School of Chemistry, University of Melbourne, Parkville, Victoria 3052, Australia

<sup>¶</sup> Department of Physics, The Flinders University of South Australia, GPO Box 2100, Adelaide, SA 5001, Australia

Received 17 March 1999, in final form 10 May 1999

**Abstract.** The technique of electron momentum spectroscopy has been employed to measure orbital momentum distributions for the complete valence electronic structure of ethylene oxide (C<sub>2</sub>H<sub>4</sub>O). The corresponding theoretical MDs were calculated using a plane wave impulse approximation model for the reaction mechanism and density functional theory for the wavefunction. Seven basis sets, at the local density approximation level and, additionally, one further that incorporated nonlocal correlation functional corrections, were studied. A critical comparison between the experimental and theoretical MDs allows us to determine the ‘optimum’ wavefunction from our basis sets. This wavefunction is then used to derive ethylene oxide’s chemically interesting molecular properties, which are subsequently compared with the results of other workers.

## 1. Introduction

The unique ability of electron momentum spectroscopy (EMS) to measure the orbital momentum distribution (MD) for binding-energy-selected electrons [1] has made it a powerful technique for evaluating the quality of theoretical wavefunctions in quantum chemistry [2, 3]. It is our thesis that it is this property of EMS, when combined with high-quality wavefunctions, as calculated using Hartree–Fock (HF) or density functional theory (DFT) procedures with sophisticated sets of basis states, that allows you to *a priori* judge the validity of the physical representation provided by a given wavefunction and hence, in turn, assess the pedigree of the molecular property information derived from that wavefunction. Supporting evidence for this notion was provided in our previous EMS/DFT studies on [1.1.1]propellane [4] and 1,3-butadiene [5]. In each case the ‘optimum’ wavefunction, as determined on the basis of a critical comparison between the experimental and theoretical MDs, was found to give the most accurate molecular property information, as assessed by comparison with results from independent measurements. Nonetheless, it is clear that further EMS/DFT studies are required before any definitive claim as to the veracity of our thesis can be made. Consequently, in this

<sup>¶</sup> Present address: Department of Physics and Astronomy, University College London, Gower Street, London WC1E 6BT, UK

paper we report the results from just such a joint study into the complete valence electronic structure for the molecule ethylene oxide ( $C_2H_4O$ ).

Ethylene oxide is a saturated three-membered ring molecule that exhibits interesting features in its molecular structure which are due, at least in part, to the strained nature of its bonds. In addition it is of considerable interest as a monomer in the polymer industry. Thus it is not surprising that its molecular properties have been widely studied by both spectroscopic and theoretical methods. The structure [6, 7], dipole moment [6], total energy [8, 9] and vibrational spectrum [10–14] have, for example, all been investigated.

The outer valence electronic structure of ethylene oxide has been previously studied with photoelectron spectroscopy (PES) using He(I) radiation by Basch *et al* [8], Schweig and Thiel [15] and Johnson *et al* [16]. In each of these studies six valence states were identified and classified as being due to the respective  $2b_2$ ,  $4a_1$ ,  $2b_1$ ,  $1a_2$ ,  $3a_1$  and  $1b_2$  orbitals. In addition, the binding energies ( $\epsilon_i$ ) of these orbitals were also accurately measured. We note that, to the best of our knowledge, no PES investigation of the inner valence  $1b_1$ ,  $2a_1$  and  $1a_1$  orbitals has been reported in the literature. We further note that the molecular orbital nomenclature that we have adopted in this paper is consistent with that employed by Schweig and Thiel [15] and Bieri *et al* [17]. From a theoretical perspective, there are currently available in the literature double-zeta quality HF wavefunction calculations for the binding energies of the relevant valence states [8, 9], the configuration interaction (CI) results of Kimura and co-workers [18] and the large atomic natural orbital (ANO) basis set calculation results of Brunger *et al* [19]. In this latter work binding energies and spectroscopic factors (see section 3), for all the valence orbitals, were obtained by using the third-order algebraic diagrammatic construction (ADC(3)) Green function method of Schirmer *et al* [20].

The only previous EMS study [19] into ethylene oxide reported experimental binding energy spectra at just two azimuthal angles,  $\phi = 0^\circ$  and  $10^\circ$  (see section 2), and theoretical MDs, within the plane-wave-impulse-approximation [1] (PWIA), using quite crude HF-level basis orbitals. The present work significantly extends that of Brunger *et al* [19] at both the experimental and theoretical levels by measuring binding energy spectra at ten azimuthal angles in the range  $\phi = 0$ – $25^\circ$ , leading to detailed experimental MDs for each respective valence orbital, and by calculating, again for each valence orbital, PWIA MDs using seven different DFT basis sets at the local density approximation (LDA) level [21]. In addition, further PWIA-DFT MDs were calculated by employing the Becke and Stoll *et al* [22–24] nonlocal correlation functional correction to the exchange-correlation energy functional.

In section 2 we briefly discuss some of the experimental aspects of the EMS technique pertaining to this work, while in section 3 details of our structure calculations are presented. Our results for the experimental and theoretical MDs are given and discussed in detail in section 4 with the molecular property information, as obtained from our ‘optimum’ theoretical wavefunction, being outlined in section 5. Finally, in section 6, conclusions from the results of the present investigation are drawn.

## 2. Experimental considerations

A detailed description of the coincidence spectrometer and multiparameter techniques used in the present EMS investigation of ethylene oxide can be found in McCarthy and Weigold [25], although we note that since their report there has been a major upgrade in the data acquisition and computer control system [4].

In the current work noncoplanar symmetric kinematics is employed with the two outgoing electrons having essentially equal energies and making equal polar angles ( $\theta = 45^\circ$ ) with respect to the incident electron beam. The incident electron energy  $E_0$  was 1000 eV plus the

binding energy  $\epsilon_i$  of the struck electron. The binding energy range of interest ( $\epsilon_i = 3\text{--}39\text{ eV}$ ) is stepped through sequentially at each of a chosen set of angles  $\phi$  ( $\phi = 0\text{--}25^\circ$ ) using a binning mode [1]. Scanning through a range of  $\phi$  is equivalent to sampling different target electron momenta  $p$  (0.16–1.90 au).

Typical binding energy spectra of ethylene oxide in the region 3–39 eV and at a total energy of 1000 eV were previously reported in Brunger *et al* [19], and so are not reproduced again here. The analysis of the measured binding energy spectra has also been described many times before [4]. Briefly, a least-squares fit to the spectra [26], assuming Gaussian profiles, is performed. The binding energies of the respective orbitals are usually fixed at the known PES values [8, 15, 16], although in this case as no PES study on the inner valence region has been reported we have employed, for them, those determined in the earlier EMS work [19], and the Gaussian widths are a convolution of the coincidence energy resolution and the natural line widths of the respective orbitals. As the coincidence energy resolution of this work, determined from measurements of the binding energy spectrum of helium, was 1.4 eV (FWHM) the fitted resolutions of the spectral peaks for  $\text{C}_2\text{H}_4\text{O}$  varied from 1.49–2.32 eV (FWHM). The area under each profile, and its uncertainty, are determined in the fit. We note at this time that it is the aforementioned limitation with our energy resolution that caused us to combine the  $2b_1$  and  $1a_2$  orbitals and the  $3a_1$  and  $1b_2$  orbitals, respectively, under single peaks in the deconvolution. To do otherwise would have raised serious questions as to the uniqueness of the fluxes (relative cross sections) derived in the fit. In addition, the ADC(3) result of Brunger *et al* [19] indicated manifold splitting and intermixing of satellite strength for the  $1b_1$  and  $2a_1$  orbitals, due to final-state configuration interaction effects, a result consistent with their binding energy spectra measurements [19]. Consequently the fluxes for these orbitals, as determined in the deconvolution, are also combined in this study.

The present angular resolution was  $\Delta\phi = 1.2^\circ$  and  $\Delta\theta = 0.6^\circ$ , as determined from the electron optics and apertures and from a consideration of the argon 3p angular correlation. Ethylene oxide (commercially purchased) of very high purity (>99.5%) was introduced into the interaction region via a variable leak valve and the EMS experiments performed.

### 3. Reaction mechanism and structure calculation details

The PWIA is used to analyse the measured cross sections for our high momentum transfer (e, 2e) collisions [1]. Using the Born–Oppenheimer approximation for the target and ion wavefunctions, the EMS differential cross section  $\sigma$ , for randomly oriented molecules and unresolved rotational and vibrations states, is given by:

$$\sigma = K \int d\Omega |\langle p \Psi_f^{N-1} | \Psi_i^N \rangle|^2, \quad (1)$$

where  $K$  is a kinematical factor which is essentially constant in the present experimental arrangement,  $\Psi_f^{N-1}$  and  $\Psi_i^N$  are the electronic many-body wavefunctions for the final ( $(N - 1)$  electron) ion and target ( $N$  electron) ground states, and  $p$  is the momentum of the electron at the instant of ionization. The  $\int d\Omega$  denotes an integral over all angles (spherical averaging) due to averaging over all initial rotational states. This is equivalent to averaging over all orientations of the molecular axis. The average over the initial vibrational state is well approximated by evaluating orbitals at the equilibrium geometry of the molecule. Final rotational and vibrational states are eliminated by closure.

The momentum space target–ion overlap  $\langle p \Psi_f^{N-1} | \Psi_i^N \rangle$  can be evaluated using configuration interaction descriptions of the many-body wavefunctions [27], but usually the weak-coupling approximation [1] is made. Here, the target–ion overlap is replaced by the

relevant orbital of, typically, the HF or Kohn–Sham [28] ground state  $\Phi_0$ , multiplied by a spectroscopic amplitude. With these approximations equation (1) reduces to:

$$\sigma = K S_j^{(f)} \int d\Omega |\phi_j(\mathbf{p})|^2, \quad (2)$$

where  $\phi_j(\mathbf{p})$  is the momentum space orbital. The spectroscopic factor  $S_j^{(f)}$  is the square of the spectroscopic amplitude for orbital  $j$  and ion state  $f$ . It satisfies the sum rule:

$$\sum_f S_j^{(f)} = 1. \quad (3)$$

Hence it may be considered as the probability of finding the one-hole configuration in the many-body wavefunction of the ion. We have previously given our ADC(3)–Green function calculation results for  $S_j^{(f)}$  in Brunger *et al* [19]. It is also possible to determine the experimental spectroscopic factors, at various binding energies  $\epsilon_i$ . This is achieved by comparison of the MD result from our PWIA calculation (using the Flinders-developed AMOLD program [1]), for a particular orbital, with that MD correspondingly derived from our measured binding energy spectra. The scaling factor to be applied to the theory, to ensure best agreement between the PWIA calculation MD and the experimental MD, is not arbitrary but is in fact the spectroscopic strength for that orbital at that binding energy.

The target–ion overlap is a one-electron function called the quasiparticle orbital. A quasiparticle equation, the Dyson equation, can be constructed from the electronic Schrödinger equations for the target and ion [27]. Formally, this is the one-electron Schrödinger equation with target and ion structure details contained in the potential operator.

The Kohn–Sham equation of DFT may be considered as an approximate quasiparticle equation, with the potential operator approximated by the exchange–correlation potential [27]. Quite recently, Duffy *et al* [29] showed that the physical significance of the valence orbitals of DFT was established by their ability to describe EMS data that are not well described by HF calculations that omit electron–correlation considerations, but are well described by full CI calculations.

In order to compute the coordinate space Kohn–Sham orbitals  $\psi_j$ , we employed DGauss, a program developed for Cray Research by Andzelm and colleagues [30,31]. DGauss is itself a part of UniChem, a suite of computational quantum chemistry programs from Oxford Molecular. Using DGauss and UniChem, we employed various basis sets [30] to build a model ethylene oxide molecule and we then minimized the energy. The molecular coordinates at the optimum geometry (minimum energy) and the Gaussian molecular orbital parameters (coefficients and exponents) were next treated as an input to AMOLD, which computes the momentum space spherically averaged molecular-structure factor [1] and the (e, 2e) cross section or MD. Note that our reasons for preferring DGauss over an alternative package such as GAUSSIAN are addressed elsewhere [40], and so are not repeated again here.

The comparisons of calculated momentum profiles with experiment (see section 4) may be viewed as an exceptionally detailed test of the quality of the basis set [2,32]. In this investigation we have used seven basis sets in the DFT computations. These basis sets are denoted by the acronyms: DZ94, DZ94P, DZVP, DZVP2, TZ94, TZ94P and TZVP. The notations DZ and TZ denote basis sets of double—or triple— $\xi$  quality. V denotes a calculation in which such a basis is used only for the valence orbitals and a minimal basis is used for the less chemically reactive orbitals. The inclusion in the basis of long-range polarization functions is represented by P.

Table 1 lists the basis sets available in DGauss for the hydrogen, carbon and oxygen atoms. We have used all of them in our calculations of ethylene oxide. The notation indicates the number of primitive Gaussians and the contraction scheme. For example, (621/41/1)



**Table 1.** Local density approximation optimized basis sets used in the DFT computations.

| Atom | DZ94     | DZ94P      | DZVP       | DZVP2      | TZ94       | TZ94P        | TZVP         |
|------|----------|------------|------------|------------|------------|--------------|--------------|
| H    | (41)     | (41)       | (41)       | (41/1)     | (311)      | (311/1)      | (3111/1)     |
| C    | (621/41) | (621/41/1) | (621/41/1) | (721/51/1) | (7111/411) | (7111/411/1) | (7111/411/1) |
| O    | (621/41) | (621/41/1) | (621/41/1) | (721/51/1) | (7111/411) | (7111/411/1) | (7111/411/1) |

means there are three contracted s, two contracted p, and one contracted d functions. The s functions consists of 6, 2 and 1 primitive Gaussians while the p functions consist of 4 and 1 primitive Gaussians. An improvement over the LDA approach to approximating the exchange-correlation functional can, in principle, be obtained by using functions that depend upon the gradient of the charge density [33]. In this study we employed the approximation to the exchange-correlation energy functional due to Becke, Stoll, Pavlidou and Preuss [22–24] (basis set marked with bspp). The nonlocal density-gradient correction for the above nonlocal model, as implemented in DGauss, was included self-consistently throughout the entire computation.

For comparison with the DFT orbitals, we have also used the HF orbitals employed previously by Brunger *et al* [19]. The first of these was the old double-zeta quality wavefunction due to Snyder and Basch [9]. The total SCF energy for this wavefunction was  $-152.801\,20\,E_H$ . The second was computed with GAMESS [34] using Dunning [35] basis sets at the triple-zeta-plus-polarization level. It employed (11s, 6p, 1d) / [5s, 3p, 1d] for each of the carbon and oxygen atoms and (5s, 1p) / [3s, 1p] for each hydrogen atom. The total SCF energy obtained for this wavefunction was  $-152.918\,05\,E_H$ , with full details being given in Brunger *et al* [19].

#### 4. Results and discussion

Binding energy spectra of ethylene oxide were measured in the region  $\epsilon_i = 3\text{--}39\text{ eV}$  and at a total energy of 1000 eV, at each of a chosen set of angles  $\phi$  (or  $p$ ). These spectra were then analysed with the least-squares-fit deconvolution technique of Bevington and Robinson [26], which allowed us to derive the required MDs for the respective valence orbitals of  $\text{C}_2\text{H}_4\text{O}$ . Although the measured momentum distributions are not absolute relative magnitudes for the different transitions are obtained [1]. In the current EMS investigation of the valence orbitals of  $\text{C}_2\text{H}_4\text{O}$ , the experimental MDs are placed on an absolute scale by summing the experimental flux for each measured  $\phi$  for the six ( $2b_2$ ,  $4a_1$ ,  $2b_1$ ,  $1a_2$ ,  $3a_1$  and  $1b_2$  orbitals) outer valence states, and then normalizing this to the corresponding sum from the result of our PWIA-DFT TZVP calculation.

In figure 1 we compare our experimental momentum distribution for the highest-occupied molecular orbital (HOMO),  $2b_2$  state at  $\epsilon_i = 10.57\text{ eV}$ , with the results of our PWIA-DFT calculations. The earlier data and PWIA-HF calculations of Brunger *et al* [19] are also shown in this figure. We note that the errors on all the present MDs, as derived during the deconvolution procedure, are one standard deviation uncertainties. It is clear from figure 1 that the measured MD for the  $2b_2$  state has very small flux at small values of  $\phi$  and a peak in the (e, 2e) cross section at  $\phi \approx 12^\circ$  ( $p \approx 0.9\text{ au}$ ), thus implying that this HOMO is p-like in nature [1]. All the theoretical PWIA-HF and PWIA-DFT results for the  $2b_2$  orbital are, in general, consistent with this observation, although it is apparent that there are differences in the details between some of the theoretical results and the experimental MD. Note that the earlier experimental results of Brunger *et al* [19] are consistent with the present data at both  $\phi = 0^\circ$  and  $\phi = 10^\circ$ ,

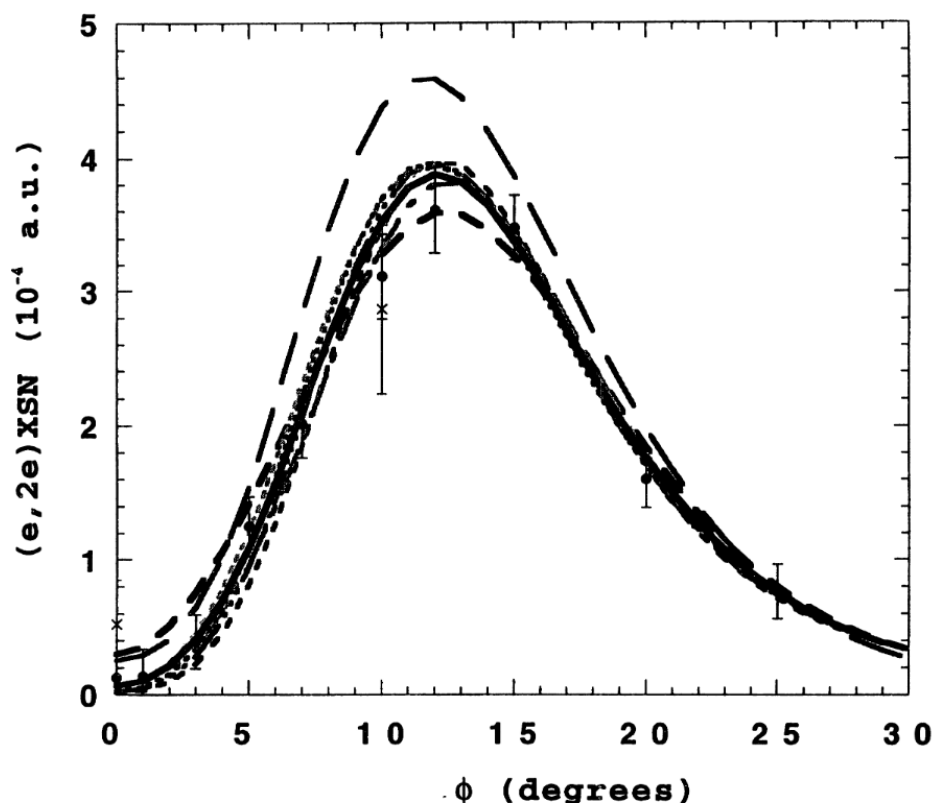


**Figure 1.** The 1000 eV noncoplanar momentum distribution for the  $2b_2$  orbital of ethylene oxide. The present experimental data ( $\bullet$ ) and the earlier result of Brunger *et al* [19] ( $\times$ ) are compared against the results of our PWIA-HF and PWIA-DFT calculations: (— — —) Snyder and Basch [9], (— — —) Brunger *et al* [19], (— · —) DZ94, (· · · · ·) DZ94P, (— · · —) DZVP, (— · · —) DZVP2, (— · · · —) TZ94, (· · · · · · ·) TZ94P.bspp, (· · · · ·) TZ94P and (—) TZVP. The acronym XSN, on the y-axis, denotes cross section.

a point which holds not just for the HOMO but for all the valence orbitals. Also note that the corresponding error bars on the present MD data points are smaller than those of Brunger *et al*, reflecting the superior statistical quality of the current binding energy spectra. There are two additional points which can be gleaned from a further consideration of figure 1. First, the PWIA-HF MD with Snyder and Basch [9] basis for the  $2b_2$  orbital is clearly inadequate, it overestimates the magnitude of the measured cross section for all  $\phi < 25^\circ$ . Secondly, for azimuthal angles in the range  $\phi \approx 9\text{--}13^\circ$ , there is a suggestion that the PWIA-DFT MDs with DZ94, TZ94, TZ94P, TZ94P.bspp and DZVP2 basis states also slightly overestimate the cross section compared with the experimental MD. However, the level of agreement between the present measurement and the corresponding  $2b_2$  theoretical MDs with DZ94P, DZVP and TZVP basis states is very good across all measured  $\phi$ , thereby making these latter basis states possible candidates for our 'optimum'  $C_2H_4O$  wavefunction.

For the next outermost valence  $4a_1$  orbital at  $\epsilon_i = 11.7$  eV, we again find that the theoretical and experimental MDs all predict that it is p-like in nature, although here the peak in the cross section is at  $\phi \approx 11^\circ$ ,  $p \approx 0.8$  au (see figure 2(a)), which is at a somewhat smaller value of momentum than was found for the  $2b_2$  orbital. For the  $4a_1$  state the PWIA-HF result using the Snyder and Basch [9] orbital again leads to an MD which is in poor agreement with that determined experimentally. Specifically, the theoretical cross section is too low in magnitude for  $\phi < 20^\circ$  and it incorrectly places the peak in the cross section to be at too high a value of momentum ( $\phi \approx 13^\circ$ ,  $p \approx 1.0$  au) compared with the experimental result (see figure 2(a)). Considering the remaining PWIA-HF MD with Dunning [35] basis of Brunger *et al* [19] and

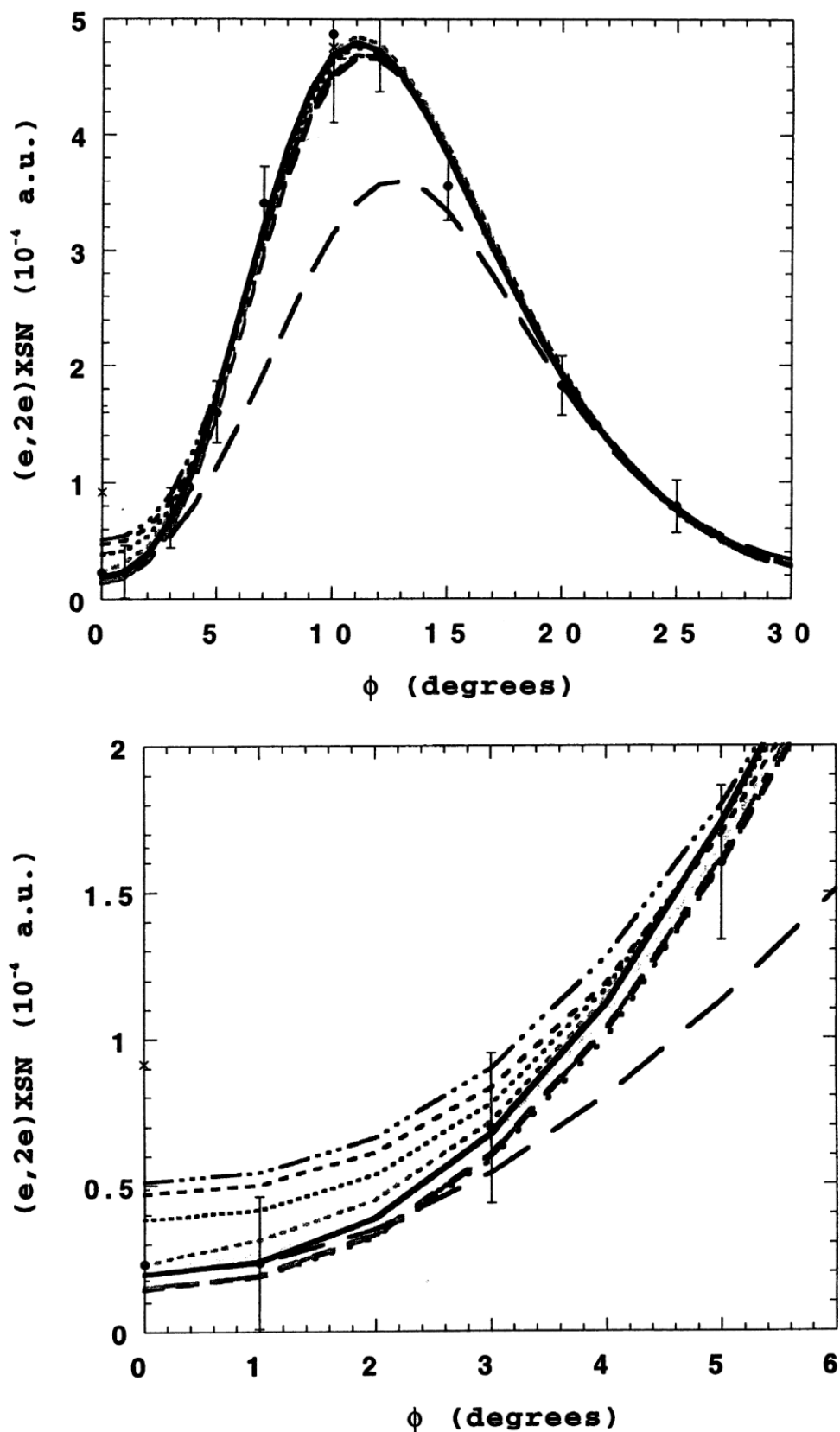


**Figure 2.** (a) The 1000 eV noncoplanar momentum distribution for the  $4a_1$  orbital of ethylene oxide. The legend is the same as figure 1. The acronym XSN, on the y-axis, denotes cross section. (b) The 1000 eV noncoplanar momentum distribution for the  $4a_1$  orbital of ethylene oxide. The legend is the same as (a), except we have restricted the azimuthal angle range to  $\phi \leq 6^\circ$  and expanded the y-axis scale. The acronym XSN, on the y-axis, denotes cross section.

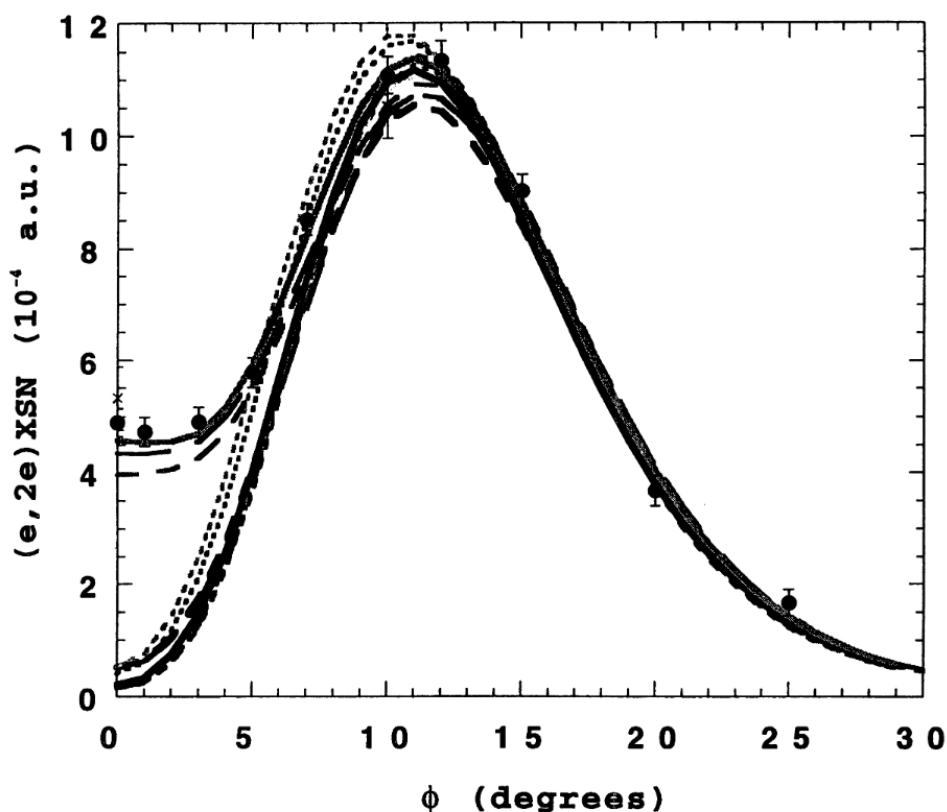


**Figure 3.** The 1000 eV noncoplanar momentum distribution for the  $2b_1 + 1a_2$  orbitals of ethylene oxide. The legend is the same as figure 1 except now the  $[0.1 \times 3a_1 + (2b_1 + 1a_2)]$  TZVP (—), Snyder and Basch [9] (---) and Brunger *et al* [19] (- - -) MDs are also additionally plotted. The acronym XSN, on the y-axis, denotes cross section.

the current PWIA-DFT MD results, then initially they all appear to be in pretty good agreement, in terms of both the shape and the magnitude of the cross section, with our experimental  $4a_1$  MD. However, in figure 2(b) we restrict the range of azimuthal angles to  $\phi \leq 6^\circ$  and expand the y-axis scale, so that it is now quite clear that at smaller values of momenta ( $\phi < 3^\circ$ ) the PWIA-DFT MD results with TZ94 and DZ94 basis states lead to cross sections that overestimate the magnitude of the (e, 2e) cross section. This observation is indicative of the sensitivity of the EMS technique for evaluating the quality of theoretical wavefunctions.

As we discussed previously, the energy resolution of the present experiment was not sufficient to enable us to resolve the  $2b_1$  orbital at  $\epsilon_i = 13.7$  eV and the  $1a_2$  orbital at  $\epsilon_i = 14.2$  eV. Thus, in figure 3 we plot the summed momentum distributions for these orbitals. In this case it is clear that all of the PWIA-HF and PWIA-DFT MD calculations fail to reproduce the experimental MD for  $\phi < 10^\circ$  ( $p < 0.76$  au), the experiment exhibiting a much stronger cross section at smaller values of momentum compared with any of the theories. This result may be an indication that none of the HF or DFT basis states are providing an adequate representation for the  $2b_1$  and  $1a_2$  orbitals. Alternatively, Brunger *et al* [19] previously canvassed and discussed the possibility of a small (10%)  $3a_1$  flux contribution to the experimental  $2b_1 + 1a_2$  MD, in that region of the binding energy spectrum. Such a contribution, while perhaps being a little speculative, is appealing as only the admixture of an s-like MD for  $\phi < 10^\circ$  could resolve the observed discrepancy between theory and experiment for the  $2b_1 + 1a_2$  MD. On allowing for this 10%  $3a_1$  admixture, we immediately see, in figure 3, that the agreement between the experimental MD and the PWIA-DFT result with TZVP basis is very good for all  $\phi$ . A similar, although not quite as spectacular, level of agreement between

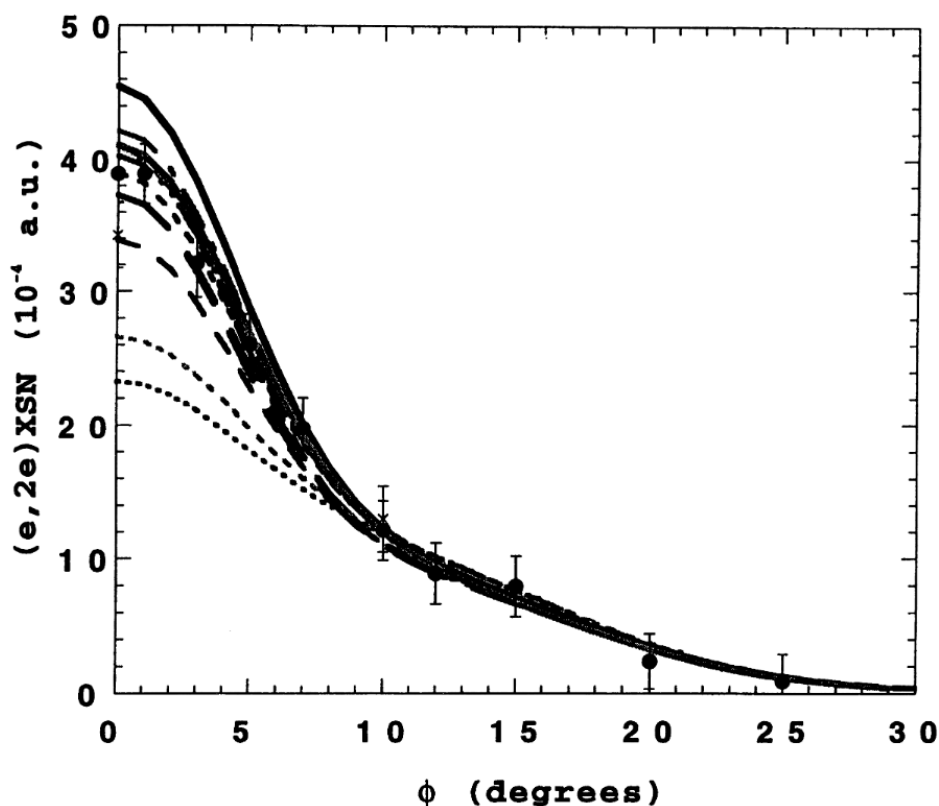


**Figure 4.** The 1000 eV noncoplanar momentum distribution for the  $3a_1 + 1b_2$  orbitals of ethylene oxide. The legend is the same as figure 1 except now the  $[0.9 \times 3a_1 + 1b_2]$  TZVP (—), Snyder and Basch [9] (---) and Brunger *et al* [19] (- - -) MDs are also additionally plotted. The acronym XSN, on the y-axis, denotes cross section.

experiment and theory is also found when the DZVP basis is employed in this fashion (not plotted). However, for the remaining basis states (Snyder and Basch [9], Brunger *et al* [19], TZ94, TZ94P, DZ94, DZ94P, TZ94P.bspp and DZVP2), even after allowing for a small  $3a_1$  flux contribution the discrepancy, to varying degrees, between the theory MDs and the measured MD remains, suggesting that there are indeed limitations with them in their representation of the  $2b_1$  and  $1a_2$  orbitals.

Although the  $3a_1$  orbital at  $\epsilon_i = 16.6$  eV and the  $1b_2$  orbital at  $\epsilon_i = 17.4$  eV are separated by 0.8 eV we cannot, as noted previously, be confident that, given our instrumental energy resolution, a unique deconvolution of the flux for these orbitals could be obtained from the fit. Consequently, in figure 4 we plot the summed experimental MD and summed momentum distributions from the PWIA-DFT and PWIA-HF calculations for the  $3a_1$  and  $1b_2$  orbitals. On considering figure 4 in more detail we initially note that the PWIA-DFT momentum distribution results with TZ94P and TZ94P.bspp basis states are in very poor agreement with the measured MD for  $\phi < 10^\circ$ . In particular, both these calculations severely underestimate the strength of the cross section at the smaller values of momentum ( $\phi$ ). Thereafter, however, the picture becomes somewhat more complicated as if there is a 10%  $3a_1$  flux contribution (see above) to the lower lying (in binding energy)  $2b_1$  and  $1a_2$  orbitals, then the PWIA theory results that we should be comparing here against the measured MD are in fact  $[0.9 \times 3a_1 + 1b_2]$ . Under these circumstances, from all the basis states we have investigated, only the PWIA-DFT MD with TZVP basis provides an excellent description of the experimental MD over all measured  $\phi$  (see figure 4). Thus, we can conclude that the TZVP basis is providing an adequate representation for the  $3a_1$  and  $1b_2$  orbitals.

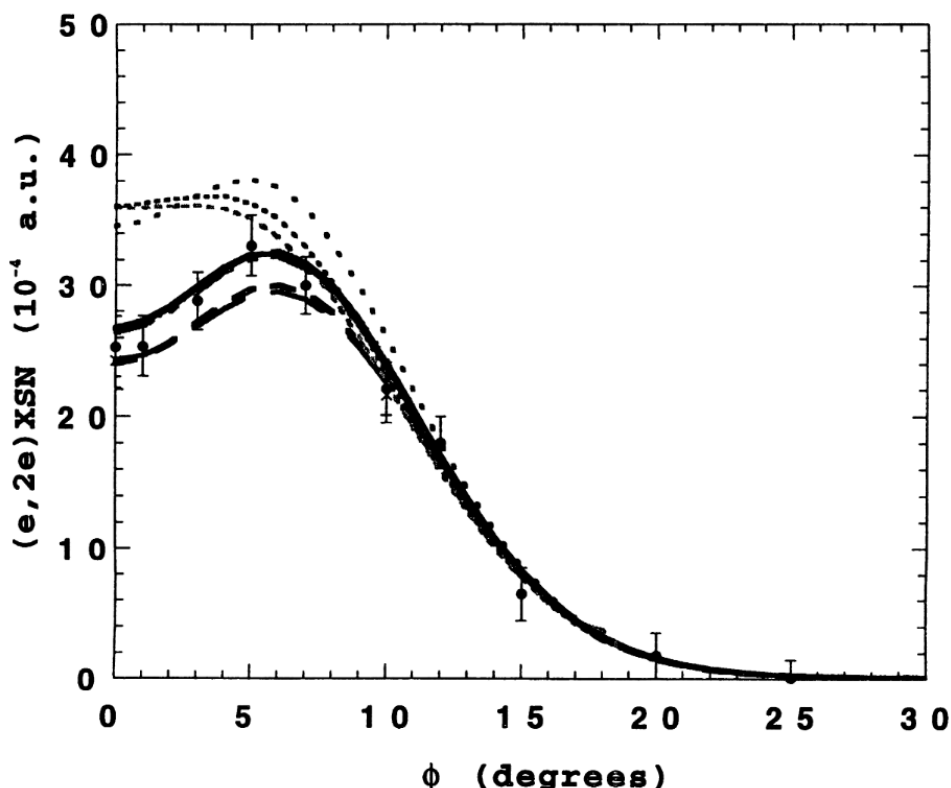


**Figure 5.** The 1000 eV noncoplanar momentum distribution for the  $1b_1 + 2a_1$  orbitals of ethylene oxide. The legend is the same as figure 1. The acronym XSN, on the y-axis, denotes cross section.

The ADC(3) calculation of Brunger *et al* [19] showed that both the  $1b_1$  and  $2a_1$  orbitals are quite severely split by final-state configuration interaction effects and that this splitting leads to overlapping spectral strength for the  $1b_1$  and  $2a_1$  orbitals. The binding energy spectra of Brunger *et al* [19] and the current binding energy spectra are consistent with this result. Thus, in figure 5 we plot the summed experimental momentum distribution for these orbitals. Also included in this figure are the respective calculated PWIA-DFT and PWIA-HF  $1b_1 + 2a_1$  momentum distributions. In this case (see figure 5) it is apparent that, to within the experimental uncertainties on the data, most of the theoretical MDs are in quite good agreement with the experimental MD over the entire range of measured  $\phi$ . Specifically, agreement between the experimental MD and the PWIA theoretical MDs was found when the HF basis states of both Snyder and Basch [9] and Brunger *et al* [19] were employed, and similarly when the DFT basis states at TZ94, DZ94, DZVP, TZVP and DZVP2 levels were also employed. Thus, figure 5 gives a good illustration of the point that, for certain orbitals, the experimental MD, with its finite uncertainties, may be somewhat insensitive as to clearly determining which of the possible basis states provide a more accurate physical picture for the orbital or orbitals in question. Having said that, we note from figure 5 that our measured MD is in disagreement with the PWIA-DFT MDs when the TZ94P, TZ94P.bspp and DZ94P basis states were respectively employed in the calculations. This clearly indicates that these latter DFT basis states are not providing a good physical representation for the  $1b_1$  and  $2a_1$  orbitals.

The innermost valence  $1a_1$  orbital is severely split into many poles, of finite spectroscopic strength, by final-state configuration interaction electron correlation effects. This is apparent from the ADC(3) calculation result and binding energy spectra of Brunger *et al* [19] and the current binding energy spectra. The energy range of the binding energy spectra in our present study ( $\epsilon_i = 3\text{--}39$  eV) was chosen to mimic that employed previously by Brunger *et al*



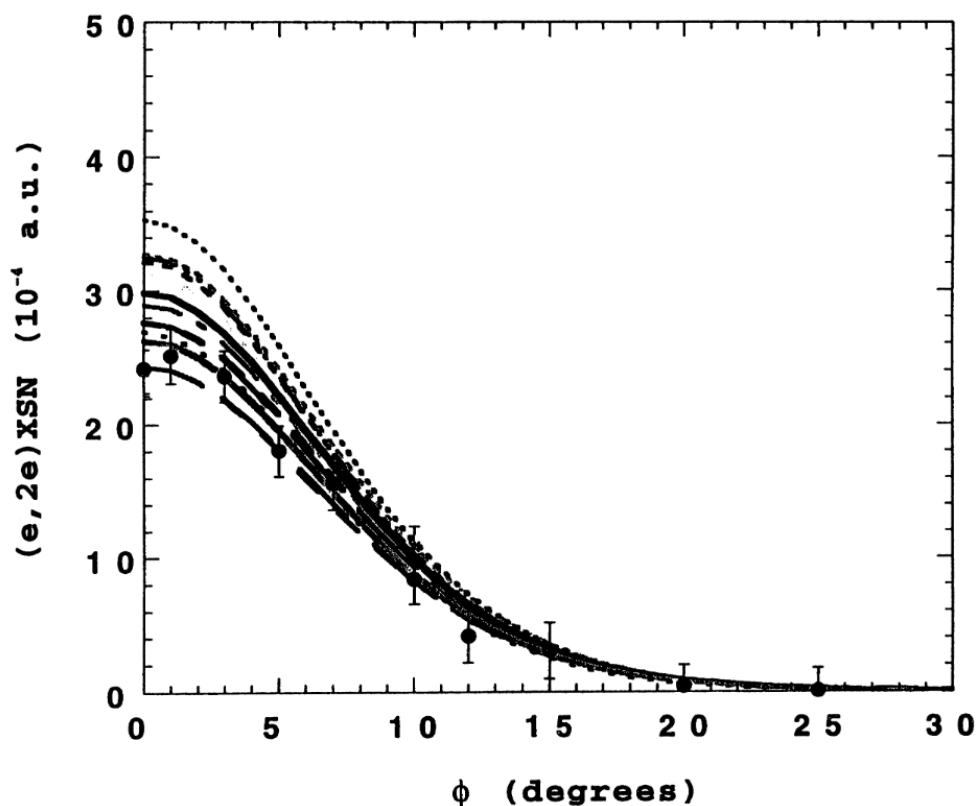


**Figure 6.** The 1000 eV noncoplanar momentum distribution for the  $1a_1$  orbital of ethylene oxide. The legend is the same as figure 1 except now the  $[0.88 \times 1a_1]$  TZVP (—), Snyder and Basch [9] (---) and Brunger *et al* [19] (-.-) MDs are also additionally plotted. The acronym XSN, on the y-axis, denotes cross section.

[19]. Consequently, we would expect that their observation for some additional ( $\sim 12\%$ )  $1a_1$  intensity existing outside this range would also be prevalent here. This is indeed found to be the case, as evidenced by acceptable agreement between the experimental MD and most of the theoretical MDs only being achieved when the latter are scaled by a factor of 0.88 (see figure 6). In particular, very good agreement with the experimental MD is found when the calculated PWIA-HF MD from Brunger *et al* [19] and the present calculated PWIA-DFT MD using TZVP basis, are respectively scaled by 0.88. This result suggests that any basis states that lead to a PWIA MD with cross section, especially for  $\phi < 5^\circ$  ( $p < 0.40$  au), greater than the PWIA-DFT TZVP result will not be in good accord with the measured MD. Such a situation occurs (see figure 6) when the following DFT basis states are utilized: DZVP2, DZ94, TZ94, TZ94P.bspp and TZ94P, and consequently we conclude that they are not providing a good description for the  $1a_1$  orbital.

In summary we can conclude that after a detailed comparison between the measured MDs, for all the respective valence orbitals of ethylene oxide, and those calculated using an extensive range of both HF and DFT basis states, only the DFT TZVP basis leads to theoretical PWIA MDs that adequately reproduce those determined experimentally. Consequently we choose the TZVP basis as our 'optimum' wavefunction for the ethylene oxide molecule. Further evidence in support of this choice can be found in table 2 which depicts the calculated total energies of  $C_2H_4O$  for each of the basis sets investigated in this paper. As the total energy  $E(E_H)$  of the TZVP result is lower (more negative) than any of the others, we can conclude that it provides the most stable configuration for the ethylene oxide molecule for all the basis states we have considered.

**Table 2.** Calculated total energies of ethylene oxide for each of the basis states studied in this investigation.

| Models                        | Total energy ( $E_H$ ) |
|-------------------------------|------------------------|
| HF: Snyder and Basch [9]      | −152.801 20            |
| HF: Brunger <i>et al</i> [19] | −152.918 05            |
| DFT: DZ94                     | −153.709 93            |
| DFT: DZ94P                    | −153.768 94            |
| DFT: DZVP                     | −153.768 64            |
| DFT: DZVP2                    | −153.780 28            |
| DFT: TZ94                     | −153.733 70            |
| DFT: TZ94P.bspp               | −152.531 75            |
| DFT: TZ94P                    | −153.753 58            |
| DFT: TZVP                     | −153.792 82            |

**Table 3.** Some molecular property information on ethylene oxide (acronyms are defined in the text).

| Property                | Experimental value     | DFT-BP/TZVP (present) |
|-------------------------|------------------------|-----------------------|
| $r_{C-C}$ (Å)           | 1.466 [6]<br>1.472 [7] | 1.476                 |
| $r_{C-O}$ (Å)           | 1.431 [6]<br>1.436 [7] | 1.444                 |
| $\angle$ HCH (°)        | 116.6 [6]<br>116.7 [7] | 115.5                 |
| $\angle$ COC (°)        | 61.7 [7]               | 61.4                  |
| $\angle$ OCH (°)        | 114.2 [7]              | 115.3                 |
| Bond order              | —                      | 1.00 (Mayer)          |
| C–C                     | —                      | 1.04 (ED)             |
| Bond order              | —                      | 0.96 (Mayer)          |
| C–O                     | —                      | 1.43 (ED)             |
| Total dipole moment (D) | 2.01 D [6]             | 2.01 D                |

## 5. Molecular property information

In tables 3 and 4 we present selected molecular property information of  $C_2H_4O$ , as obtained from the calculated wavefunction, for our DFT-BP/TZVP model. Also included in these tables are relevant experimental values for these same quantities as measured in independent experiments.

Scheiner *et al* [33] quite recently explored the dependence of molecular energies and other properties on the DFT basis set and density functionals, with the conclusions they drew being quite elucidatory in the context of the current work. They calculated an extensive range of molecular properties for a considerable number of molecules and compared these results to ‘known’ values from experimental measurements. On the basis of this comparison they then drew some conclusions, two of which, with specific regard to the basis set dependence of the Kohn–Sham equation using several density functionals, we now highlight. First, they found the choice of basis set was crucial to the quality of the derived molecular property information. Specifically, they noted that for high accuracy, large basis sets of at least TZ quality augmented with polarization functions are needed. This was particularly true for the calculation of dipole moments where both Becke–Perdew [22, 23, 36] (BP) and Becke–Lee–Yang and Parr [22, 23, 37] (BLYP) nonlocal corrections were also required for accurate

**Table 4.** Vibrational spectrum of ethylene oxide.

| Observed [12, 13]<br>frequency (cm <sup>-1</sup> ) | Observed [6, 7]<br>intensity (%) | DFT-BP/TZVP<br>frequency (cm <sup>-1</sup> ) | DFT-BP/TZVP<br>intensity (%) |      |
|--|----------------------------------|--|------------------------------|------|
| 808  | { 42 ± 2                         | 795  | 5                            | { 40 |
| 822  |                                  | 820  | 0                            |      |
| 877  |                                  | 893  | 35                           |      |
| 1020   | { 3                              | 1013   | 0                            | { 3  |
| —  |                                  | 1114   | 0                            |      |
| 1120   |                                  | 1121   | 0                            |      |
| 1147   |                                  | 1131   | 0                            |      |
| 1159   |                                  | 1166   | 2                            |      |
| 1270   | 8 ± 0.3                          | 1256   | 6                            |      |
| 1470   | 0                                | 1465   | 0                            |      |
| 1497   | 1 ± 0.2                          | 1495   | 1                            |      |
| 2978   | 26 ± 4                           | 3009   | 18                           |      |
| 3005   | 5 ± 2                            | 3013   | 9                            |      |
| —  |                                  | 3087   | 0                            |      |
| 3065   | 22 ± 3                           | 3103   | 21                           |      |

results. Second, for the reaction energies and molecular geometries of the first and second row molecular systems they investigated, the BP nonlocal correlation functional was found to give a superior overall performance compared with that of the BLYP correction. The results we obtained from our previous EMS study on 1,3-butadiene [5], which examined in detail these same issues, were entirely consistent with the observations of Scheiner *et al* [33], in spite of the calculated MDs not being as sensitive to the choice of the nonlocal correlation functional correction (bspp, BP or BLYP) as we would have liked. Thus, in tables 3 and 4 the molecular property information we present are derived from our 'optimum' TZVP basis with BP correction.

The calculated C<sub>2</sub>H<sub>4</sub>O structure is compared with two experimentally derived structures in table 3. There is good agreement between the measured [6, 7] and calculated bond length values for the heavy atoms with average deviations being generally less than 0.01 Å. The angles between the heavy atoms were in excellent agreement with the experimental values, the calculated and observed [6, 7] HCH and OCH angles only disagreed by slightly more than 1°. The calculated and measured [6] values for the total dipole moment (in units of Debyes, D) were both 2.01 D, although such a high level of agreement is probably somewhat fortuitous.

We also investigated the electron density in the bonding regions of ethylene oxide. We carried out a study analogous to that of Wiberg and co-workers [38, 39], to estimate the electron density ( $\rho_b$ ) at the bond critical point [39] (midway between the two atoms). We obtained a value of  $\rho_b = 0.240 a_0^{-3}$  for the C–C density and  $0.260 a_0^{-3}$  for the C–O density. We used Wiberg's empirical method to calculate bond orders from DFT electron densities at the bond critical points. The electron densities at the bond critical points of the model compounds ethane, ethene, ethyne and benzene (respective bond orders of 1.0, 2.0, 3.0 and 1.5) were used to determine the constants in the relation between bond order  $n$  and the bond critical point electron densities  $\rho_b$  [39]:

$$n = \exp[7.075(\rho_b - 0.2377)]. \quad (4)$$

This relationship yielded ethylene oxide bond orders of 1.04 for the C–C bonds and 1.43 for the C–O bonds (see table 3). We also calculated the bond orders using Mayer population analysis. The C–C bond order of 1.00 and the C–O bond order of 0.96 were in fair agreement with our values derived from the bond critical point electron densities.

The infrared spectra of  $\text{C}_2\text{H}_4\text{O}$  and  $\text{C}_2\text{D}_4\text{O}$  are very complicated with almost all the fundamental bands overlapping one another. This affects accurate measurements of vibrational frequencies and the interpretation of individual bond intensities. Studies of the vibrational spectrum of  $\text{C}_2\text{H}_4\text{O}$  have been reported by several groups. Nakanaga [12, 13] reported the infrared (IR) absorption intensities of ethylene oxide and ethylene oxide- $\text{d}_4$  in the gas phase and compared these with the results of a CNDO/2 calculation. Spiekermann *et al* [14] carried out similar studies in the gas phase and reported the absolute IR intensities. From our 'optimum' DFT-BP/TZVP calculations we were also able to calculate the frequencies of the vibrational modes of  $\text{C}_2\text{H}_4\text{O}$  with reasonable accuracy, as is summarized in table 4. In addition (again see table 4), the calculated intensities of the transitions are in reasonable agreement with the observed experimental infrared spectra.

## 6. Conclusions

We have reported on MD measurements for the complete valence electronic structure of ethylene oxide. The MD measurements were compared against an extensive series of calculations using both HF and DFT basis sets, the latter not only being at the LDA level but also in one case incorporating the bspp nonlocal correlation functional correction. On the basis of this comparison between the experimental and theoretical MDs, we found the TZVP basis set provided the most physically reasonable representation of the ethylene oxide wavefunction. This result is consistent with the findings of the quite general investigation of Scheiner *et al* [33]. Molecular property information derived, from the calculations using the DFT-BP/TZVP model, were found to be in good agreement with the available results from independent measurements. This finding, when coupled with the results from our EMS studies on [1.1.1]propellane and 1,3-butadiene [5], clearly demonstrates the usefulness of EMS in *a priori* basis set evaluation and, as a consequence, in determining reliable molecular property information for the molecule in question.

## Acknowledgments

We thank Professors I E McCarthy and E Weigold for their continued support of our endeavours. MJB acknowledges the Australian Research Council for his Fellowship, while MTM and DAW thank the CSIRO Divisions of Mathematical and Information Sciences and Molecular Science for travel support. MJB also thanks Dr W R Newell and his colleagues for their hospitality during his visit to University College London.

## References

- [1] McCarthy I E and Weigold E 1991 *Rep. Prog. Phys.* **54** 789
- [2] Bawagan A, Brion C E, Davidson E R and Feller D 1987 *Chem. Phys.* **113** 19
- [3] Coplan M A, Moore J H and Doering J P 1994 *Rev. Mod. Phys.* **66** 985
- [4] Adcock W, Brunger M J, Clark C I, McCarthy I E, Michalewicz M T, von Niesen W, Weigold E and Winkler D A 1997 *J. Am. Chem. Soc.* **119** 2896
- [5] Brunger M J, Winkler D A, Michalewicz M T and Weigold E 1998 *J. Chem. Phys.* **108** 1859
- [6] Landolt-Börnstein 1976 *Structure Data of Free Polyatomic Molecules* vol 7 (Berlin: Springer) p 185
- [7] Cunningham G L, Boyd A W, Myers R J, Gwinn W D and Le Van W I 1951 *J. Chem. Phys.* **19** 676
- [8] Basch H, Robin M B, Kuebler N A, Baker C and Turner D W 1969 *J. Chem. Phys.* **51** 52
- [9] Snyder L C and Basch H 1972 *Molecular Wavefunctions and Properties* (New York: Wiley) p 256
- [10] Cant N W and Armstead W J 1975 *Spectrochim. Acta A* **31** 839
- [11] Bertie J E and Othen D A 1973 *Can. J. Chem.* **51** 1155

- [12] Nakanaga T 1981 *J. Chem. Phys.* **74** 5384
- [13] Nakanaga T 1980 *J. Chem. Phys.* **73** 5451
- [14] Spiekermann M, Bougeard D and Schrader B 1982 *J. Comput. Chem.* **3** 354
- [15] Schweig A and Thiel W 1973 *Chem. Phys. Lett.* **21** 541
- [16] Johnson K, Powis I and Danby C J 1982 *Chem. Phys.* **70** 329
- [17] Bieri G, Burger F, Heilbronner E and Maier J P 1977 *Helv. Chim. Acta.* **60** 2213
- [18] Kimura K, Katsumata S, Achiba Y, Yamazaki T and Iwata S 1981 *Handbook of He(I) Photoelectron Spectra of Fundamental Organic Molecules* (New York: Halsted)
- [19] Brunger M J, Weigold E and von Niessen W 1995 *Chem. Phys. Lett.* **233** 214
- [20] Schirmer J, Cederbaum L S and Walter O 1983 *Phys. Rev. A* **28** 1237
- [21] Nesbet R K 1996 *J. Phys. B: At. Mol. Opt. Phys.* **29** 173
- [22] Becke A D 1988 *Phys. Rev. A* **38** 3098
- [23] Becke A D 1988 *J. Chem. Phys.* **88** 2547
- [24] Stoll H, Pavlidou C M E and Preuss H 1978 *Theor. Chim. Acta* **49** 143
- [25] McCarthy I E and Weigold E 1988 *Rep. Prog. Phys.* **51** 299
- [26] Bevington P R and Robinson D K 1990 *Data Reduction and Error Analysis for the Physical Sciences* (New York: McGraw-Hill)
- [27] Casida M 1995 *Phys. Rev. A* **51** 2005
- [28] Kohn W and Sham L J 1965 *Phys. Rev. A* **140** 1133
- [29] Duffy P, Chong D P, Casida M and Salahub D R 1994 *Phys. Rev. A* **50** 4707
- [30] Andzelm J and Wimmer E 1992 *J. Chem. Phys.* **96** 1290
- [31] Komornicki A and Fitzgerald G J 1993 *J. Chem. Phys.* **98** 1398
- [32] Adcock W, Brunger M J, Michalewicz M T and Winkler D A 1998 *Austral. J. Phys.* **51** 707
- [33] Scheiner A C, Baker J and Andzelm J W 1997 *J. Comput. Chem.* **18** 775
- [34] Schmidt M, Baldridge K K, Boatz J A, Jensen J H, Koseki S, Gordon M, Nguyen K A, Windurs T L and Elbert S T 1984 *QCPE Bull.* **14** 52
- [35] Dunning T H 1971 *J. Chem. Phys.* **55** 716
- [36] Perdew J P 1986 *Phys. Rev. B* **33** 8822
- [37] Lee C, Parr R G and Yang W 1988 *Phys. Rev. B* **37** 785
- [38] Wiberg K B, Bader R F W and Lau C D H 1987 *J. Am. Chem. Soc.* **109** 985
- [39] Wiberg K B, Bader R F W and Lau C D H 1987 *J. Am. Chem. Soc.* **109** 1001
- [40] Michalewicz M T, Brunger M J, McCarthy I E and Norling V M 1995 *CRAY Users Group 1995 Fall Proceedings (Alaska)* ed R Shaginaw pp 37–41